한국동력기계공학회지 제20권 제2호 pp. 58-65 2016년 4월 ISSN 1226-7813(Print) ISSN 2384-1354(Online)
Journal of the Korean Society for Power System Engineering http://dx.doi.org/10.9726/kspse.2016.20.2.058
Vol. 20, No. 2, pp. 58-65, April 2016

Dynamics Identification and Robust Control Performance Evaluation of Towing Rope under Rope Length Variation

Anh-Minh D. Tran* and Young-Bok Kim**†

(Received 3 February 2016, Revision received 19 February 2016, Accepted 22 February 2016)

Abstract: Lately, tugboats are widely used to maneuver vessels by pushing or towing them where tugboats use rope. In order to correctly control the motion of tugboat and towed vessel, the dynamics of the towline would be well identified. In real application environment, the towing rope length changes and the towing load is not constant due to the various sizes of towed vessel. And there are many ropes made by many types of materials. It means that it is not easy to obtain rope dynamics, such that it is too difficult to satisfy the given control purpose by designing control system. Thus real time identification or adaptive control system design method may be a solution. However it is necessary to secure sufficient information about rope dynamics to obtain desirable control performance. In this paper, the authors try to have several rope dynamic models by changing the rope length to consider real application conditions. Among them, a representative model is selected and the others are considered as uncertain models which are considered in control system design. The authors design a robust control to cope with strong uncertain and nonlinear property included in the real plant. The designed control system based on robust control framework is evaluated by simulation.

Key Words : Rope, Dynamic Identification, Rope Length, Nonlinearity, Robust Control, Control Performance

1. Introduction

Towing rope has vast range of applications. Tugboats tow marine structure to the required site in the sea, tanker in salvage operation and move ships in a crowded harbor to a narrow canal using rope. In addition, towing system is also used for delivering dredged sand, offshore crane, construction materials, and so on. Some tugboats serve as ice breakers. Fig. 1 shows the applications of towing rope.

However the towing operations become critical when it runs in harsh environmental condition. There were some collision accidents due to towline broken. For example, on 7th December 2007, the tanker Hebei Spirit was struck by the ocean crane barge. So many researchers through the world have studied about towline dynamics[1~3]. Their basic approaches are similarly based on the finite element method (FEM).

Aamo et al.[1] derived a new finite element model of the cable suspended in water. In this study, Morison's equation was used to model the hydrodynamic loads on the cable. Yoon et al.[2] subdivided towing rope into multiple finite elements.

**† Young-Bok Kim (corresponding author): Department of Mechanical System Engineering, Pukyong National University.
E-mail: kpjiwoo@pknu.ac.kr, Tel: 051-629-6197
*Anh-Minh D. Tran: Department of Control and Mechanical Engineering, the Graduate School, Pukyong National University.

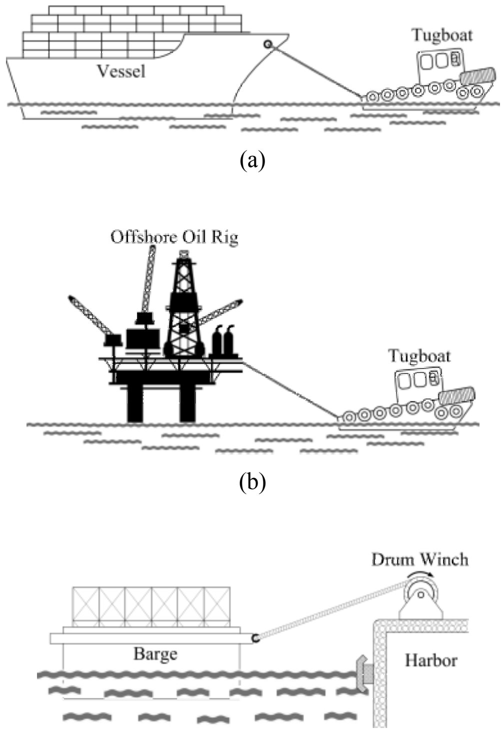

(c)

Fig. 1 Applications of towing rope

They considered five-degree-of-freedom equations of motion except roll. Kaminski et al.[3] applied Rigid Finite Element Method to obtain a model of rope including its elastic and dissipative properties. Kim[4] studied motion control problem with mooring ropes. In this study, rope dynamics is not considered. Nam et al.[5] derived only towing force when a vessel is towed by tugboat without considering rope dynamic characteristics.

However, the research results on this topic have been limited mostly to theoretical study. For examples, the high fidelity models were obtained such that these results are not suited for control system design and real applications if the rope length and load on the rope are changed in real time. Especially, in the ship berthing operation, a ship moves to the quay area from several meter apart by a mooring winch and cable where key issue is rope tension control. In this case, the winch is fixed and the rope length is varied such that the static and dynamic property of rope might be varied in the wide range also. If we consider the uncertain and nonlinear characteristics in control system design, it is necessary to find out something good solution. For this, the authors try to design a robust control system to cope with strong uncertainties etc. In this study, the actuator and rope models are obtained from experiments by varying the rope length. Especially, to obtain rope dynamic characteristics, the towing rope is excited by chirp signal such that the data including control voltage, motor current, and tension are collected. After that low order actuator and rope models are identified, a robust controller is designed to cope with perturbed rope models. Finally, nonlinear models are used to evaluate the performance of proposed control method.

2. Modeling

2.1 Experiment setup

The experimental set-up is illustrated in Fig. 2 and Fig. 3. The system used in experimental apparatus consists of motor driver, DC motor, pulleys, loadcell and amplifier. The data acquisition program is implemented in LabVIEW language 9.0. The system hardware for data acquisition is NI USB-6259. Table 1 shows the specifications of the experiment apparatus.

Table 1 Specification of experimental apparatus

Motor Voltage [V] Rated current [A] Rated speed [RPM] Rated power [W]	Maxon 24 2 6910 48
Reduction gear Ratio	28:1
Loadcell	CASKOREA SBA-50L
Transducer Amplifier	CASKOREA LCT-II

(a) photo of overall tension control system

(b) loadcell installed on the opposite end side

(c) actuator system for tension control with loadcell

Fig. 2 Photos of experimental apparatus

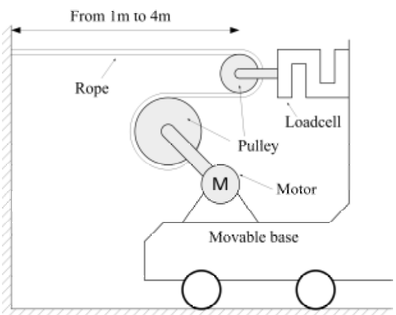

Fig. 3 Schematic diagram of actuator part

2.2 Data acquiring

In this step, sweep sinusoidal chirp signal of frequency varying (from 1 Hz to 20 Hz in a sweep time of around 10 seconds) is sent to the actuator such that the rope tension is increased and decreased. Actual current in motor and tension force measured by loadcell are recorded. We also changed the length of cable from 1m to 4m, and collected the corresponding data. Fig. 4 shows an example of experimental data.

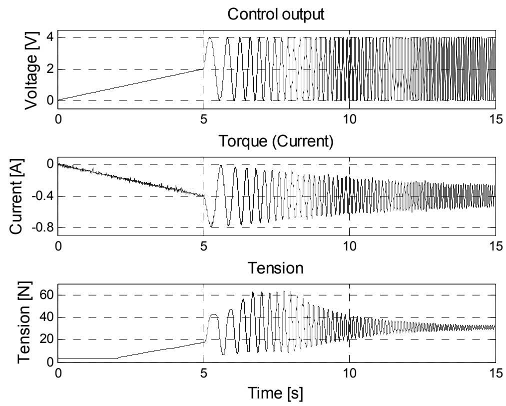

Fig. 4 Chirp signal response of system

2.3 Developing plant models from experiment data

In this study, actuator and rope model are identified individually and represented as transfer functions.

2.3.1 Actuator (Driver and Motor)

Using the motor control signal (voltage) and motor current as output signal, we first estimate a linear dynamic model for the actuator as a linear transfer function.

For parameter estimation with specified model orders, we predefine the number of poles, zeros and delay term (or dead time). Using System Identification Toolbox in MATLAB, then their poles and zeros locations to maximize the fit rate with the selected data sets are automatically derived.

Fig. 5 shows the similarity between experiment result for real plant and simulation results obtained by specifying poles and zeros. Where (a) shows the similarity between the linear models and real plant, and (b) is the similarity between the nonlinear models and real plant. The numerically calculated fitting rates in two systems are summarized in Table 2.

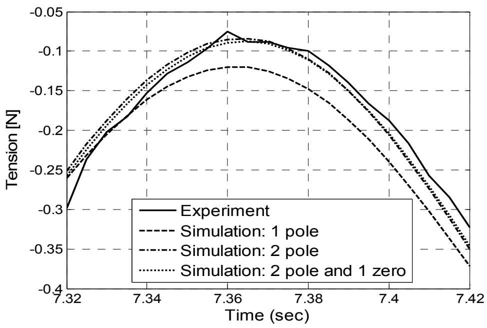

(a) simulation results for linear models and experiment result

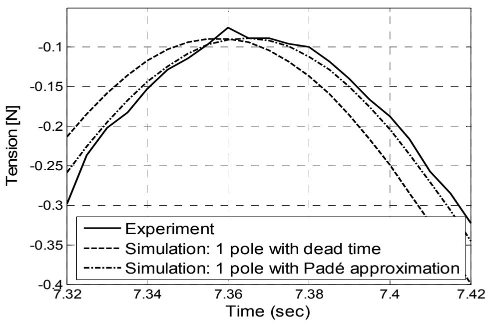

(b) simulation results for nonlinear models with delay term and experiment result

Fig. 5 Experimental data and simulation result for actuator models

Table 2 Fitting ratio of various actuator models for the real plant

Model	Fitting ratio (%)
1 pole	84.10
2 pole	95.22
2 poles and 1 zero	95.65
1 pole with dead time	95.65
1 pole with Padé approximation	95.66

In this study, we choose first order transfer function with delay time as an actuator model given as follows:

$$P_a = \left(\frac{-6.2}{s+30.9}\right)e^{-0.007s} \tag{1}$$

then a nominal model candidate is selected as following equation.

$$P_{nom\_a} = \frac{-6.2}{s+30.9} \tag{2}$$

And the first-order Padé approximation of delay term in Eq. (1) is obtained as follows:

$$P_a \approx \left(\frac{-6.2}{s+30.9}\right)\left(\frac{-s+286}{s+286}\right) \tag{3}$$

2.3.2 Towing rope

A linear dynamic model of the rope is calculated from the data which are measured from the two loadcells installed on the actuator part ((c) in Fig. 2) and opposite part ((b) in Fig. 2).

For parameter estimation of the given linear models, the authors obtained experimental data by changing the rope length from 1 to 4 meter.

Let's define a basic model as follows:

$$P_c = \frac{b_0 s^3 + b_1 s^2 + b_2 s + b_3}{s^4 + a_1 s^3 + a_2 s^2 + a_3 s + a_4} \tag{4}$$

Using the data obtained by changing the length of cable from 1m to 4 m, the parameters of transfer function of rope shown in Eq. (4) are estimated by using MATLAB Identification Toolbox, and summarized in Table 3.

It is clear that the parameter values strongly depend on rope length variation. Then we take a nominal model using the nominal values represented in Table 3. Based on the nominal values, parameter variations are considered as uncertainties which will be used in designing robust control system.

Table 3 Estimated parameter values of Eq. (4)

Length (m)	b_0	b_1	b_2	b_3
1	825.1	-42400	-26670	-15420
2	499.8	-38780	-29900	-8802
3	296.5	-25880	-24060	-5394
4	248.2	-19590	-15870	-5241
Minimum value	248.2	-42400	-29900	-15420
Maximum value	825.1	-19590	-15870	-5241
Nominal value	**536.7**	**-30995**	**-22885**	**-10330.5**
Variation [%]	54	37	31	49

Length (m)	a_1	a_2	a_3	a_4
1	24.33	858	350.9	208.5
2	22.19	635.3	274.4	116.1
3	14.89	440.3	214.9	74.58
4	11.8	304.4	143.6	67.45
Minimum value	11.8	304.4	143.6	67.45
Maximum value	24.33	858	350.9	208.5
Nominal value	**18.1**	**581.2**	**247.3**	**138**
Variation [%]	34	48	42	51

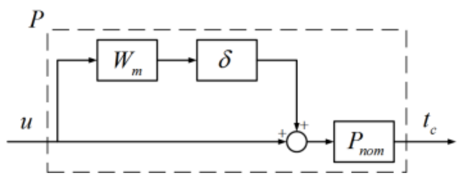

Fig. 6 Block diagram of the perturbed plant

3. Controller design

For designing robust control system, unmodelled dynamics, neglected nonlinearities and system parameter variations should be considered. Then the uncertainties derived and represented in section 2 are approximated and introduced as input multiplicative uncertainty which gives rise to the perturbed transfer function:

$$P = P_{nom}\left(1 + W_m \delta\right) \tag{5}$$

which can be depicted in Fig. 6 [6-7]. In Eq. (5) and Fig. 11, P_{nom} is the nominal plant, W_m is the uncertainty weight function, and δ presents the uncertainty bound on magnitude of the family of plants, $|\delta| \le 1$. In general, the uncertainty weight function W_m is chosen as follows:

$$\frac{\left|P(j\omega) - P_{nom}(j\omega)\right|}{\left|P_{nom}(j\omega)\right|} < \left|W_m(j\omega)\right| \tag{6}$$

Where W_m is found graphically as shown in Fig. 7 and then approximated by fourth-order transfer function. As a result, we obtain

$$W_m = \frac{2.382s^4 + 272.9s^3 + 3471s^2 + 21600s + 905.1}{s^4 + 416.7s^3 + 4962s^2 + 73970s + 19380} \tag{7}$$

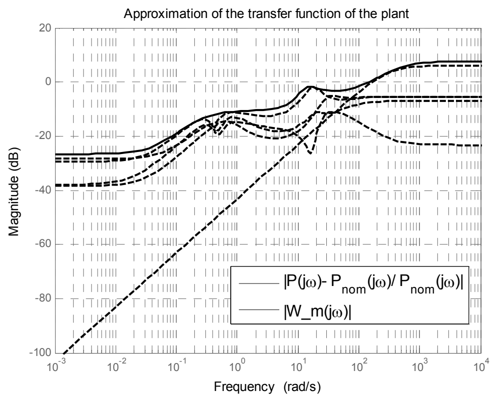

Fig. 7 Plant uncertainty approximation

Let the inputs and outputs of the uncertain blocks δ be denoted by y_m and u_m, respectively. We can arrange the actuator model as

$$\begin{bmatrix} y_m \\ t_m \end{bmatrix} = P_{LFT} \begin{bmatrix} u_m \\ u \end{bmatrix} \tag{8}$$

$$u_m = \delta y_m . \tag{9}$$

Where,

$$P_{LFT} = \begin{bmatrix} 0 & W_m \\ P_{nom} & P_{nom} \end{bmatrix} \tag{10}$$

Based on these facts abovementioned, a configuration for control system design is illustrated in Fig. 8. Where P is family of plant with the uncertainty, and K is controller. And r, y, u, e, d

represent reference input, output, control, error signal and disturbance, respectively.

The goal of control system design is to find a controller K which ensures the stability and good control performance under the defined constraint.

And the robust stability and desirable control performance for all possible family of plant with the control input constraint should be achieved. According to the H_∞ frame work, the control weighting function W_u is introduced to satisfy the constraint on the control signal u which does not surpass a power output, and the performance weight function W_p is used to ensure robust stability and robust performance. It is well known fact that choosing the weighting functions is a crucial step in robust control design. And they are chosen to represent the frequency characteristics of some external disturbances and the requirement level of performance including the consideration of control-effort constraint. The control scheme with weighting functions is illustrated in Fig. 8.

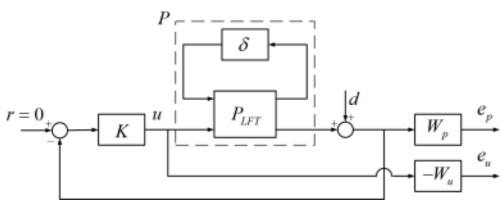

Fig. 8 Control system configuration based on H_∞ control framework

In general, the controller K is designed to minimize the transfer function T_{ed} from d to e as small as possible, then it can be represented as follows:

$$\|T_{ed}\|_\infty = \left\| \begin{matrix} W_p(I+PK)^{-1} \\ W_u K(I+PK)^{-1} \end{matrix} \right\|_\infty < 1 \tag{11}$$

Then a controller satisfying the condition given in Eq. (11) can be easily calculated by using the robust control toolbox in MATLAB [7-8]. After extensive several trials, the weighting functions for designing a control system are chosen as follows:

$$W_u = 0.1,\ W_p = \frac{0.0005s + 0.005}{0.7s + 0.0001} \tag{12}$$

With the chosen weighting functions given In Eq. (12) and using the MATLAB Robust Control Toolbox with *hinfsys* function, the controller K is calculated and reduced order one is obtained as follows:

$$K = \frac{0.0069s^3 + 6.7452s^2 + 2.8952s + 1.6333}{100s^3 + 64.9255s^2 + 27.6986s + 0.004} \tag{13}$$

4. Simulation

In this section, the authors present simulation results. The robust controller designed above is used to control the tension of rope. The simulation diagram is depicted in Fig. 9.

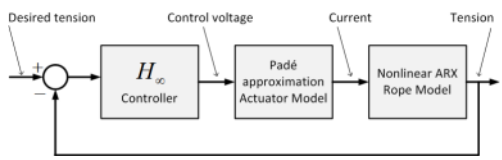

Fig. 9 Simulation diagram

To show a simple comparison example, the authors examine a PID controller given as follows:

$$K_{PID} = k_P + k_I \frac{1}{s} + k_D \frac{k_N}{1 + k_N \frac{1}{s}} \tag{14}$$

Then the optimum parameters are chosen as follows:

Proportional gain: $k_P = 0.0212$

Integral gain: $k_i = 0.0818$

Derivative gain: $k_D = -0.013$

Filter coefficient: $k_N = 1.6275$

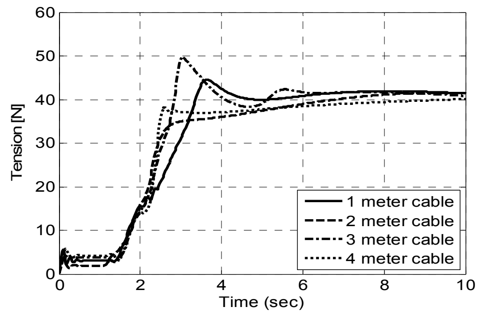

(a) target is 40N

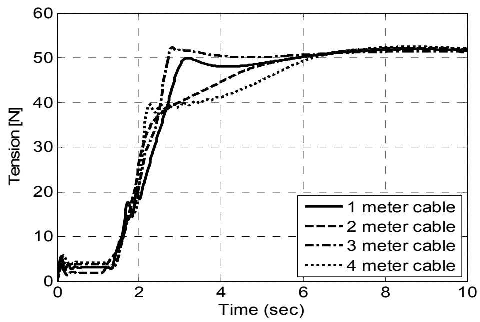

(b) target is 50N

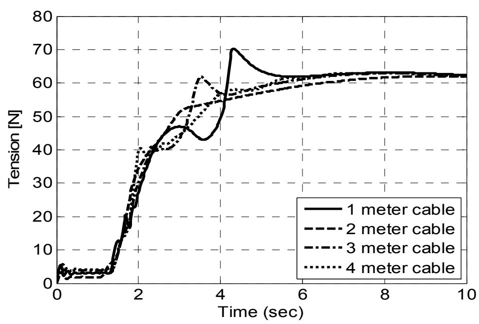

(c) target is 60N

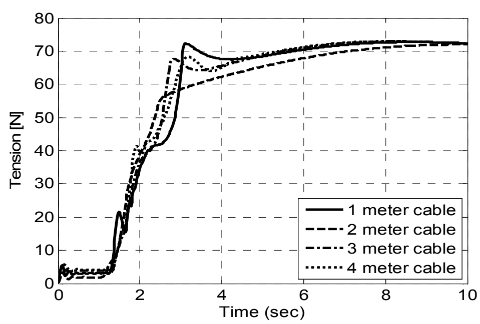

(d) target is 70N

Fig. 10 Step responses with robust control

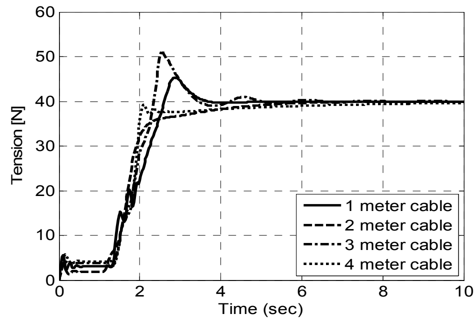

(a) target is 40N

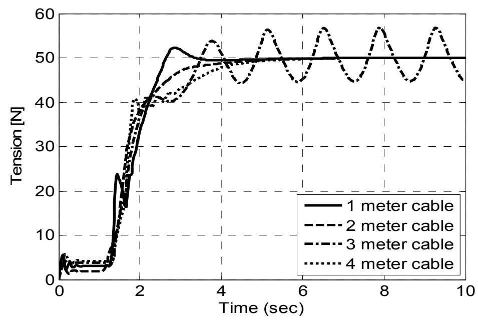

(b) target is 50N

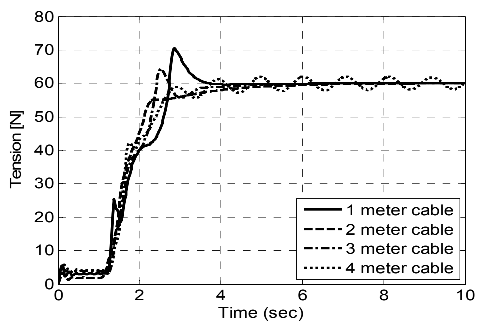

(c) target is 60N

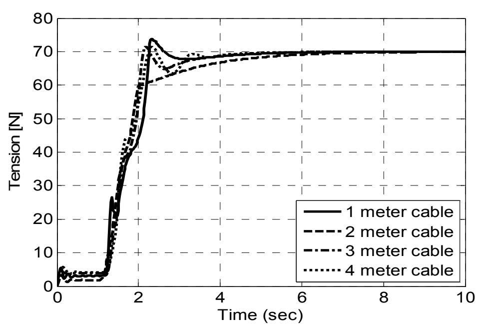

(d) target is 70N

Fig. 11 Step responses with PID control

The corresponding simulation results are shown in Fig. 10 and Fig. 11 which represent tension control performance for the different targets (40, 50, 60 and 70N) with varying cable(rope) length (1, 2, 3, and 4m).

From the simple comparison results, the robust control gives better performance than PID scheme.

However, in the transient responses, it may be said that good control responses do not be kept due to the cable length variation etc.

5. Conclusion

In this paper, a practical towing rope modeling method was tried. For this purpose, the dynamic properties of towing rope were measured and analyzed through several experiments by winding and unwinding the rope. From the experiment and simulation results, representative model of actuator and rope were obtained, respectively. Based on the nominal model, parameter variations and nonlinear properties are considered as uncertainty. By designing the robust control system, the authors tried to obtain something desirable control performance in tough condition. However, as described in previous, it is difficult to obtain good control performance especially in transient response. If a control system exposes to varying rope length and strong nonlinear property, it is clearly hard to keep good control performance continuously in the wide operating range.

Therefore, the authors will introduce switching control and gain-scheduling control method to cope with rope length variation in future study.

Acknowledgement

This work was supported by a Research Grant of Pukyong National University(2015Year)

References

1. O. M. Aamo and T. I. Fossen, 2000, “Finite Element Modelling of Mooring Lines”, Mathematics and Computers in Simulation, Vol. 53, pp. 415-422.
2. H. K. Yoon, H. S. Lee, J. K. Park and Y. G. Kim, 2012, “Dynamic Modeling and Simulation of a Towing Rope using Multiple Finite Element Method”, Journal of Navigation and Port Research, Vol. 36, No. 5, pp. 339-347.
3. H. Kaminski and P. Fritzkowski, 2013, “Application of the Rigid Finite Element Method to Modelling Mopes”, Latin American Journal of Solids and Structures, Vol. 10, No. 1, pp. 91-99.
4. Y. B. Kim, 2013, “A Positioning Mooring System Design for Barge Ship Based on PID Control Approach”, Journal of the Korean Society for Power System Engineering, Vol. 17, No. 5, pp. 94-99.
5. T. K. Nam, C. H. Jung, J. M. Kim and H. J. Choi, 2014, “A Study on the Calculation of Towing Force for the Disabled Ship and Its Experiments”, Journal of Navigation and Port Research, 2014, Vol. 38, No. 5, pp. 463-470.
6. D. C. Dang, C. N. Kang and Y. B. Kim, 2015, “Robust Control System Design for Robot Motion Regeneration under Disturbance Input”, Journal of Drive and Control, Vol. 12, No. 3, pp. 1-10.
7. D. W. Gu, P. H. Petrov and M. M. Konstantinov, 2005, Robust Control Design with MATLAB, Springer.
8. R. Y. Chiang and M. G. Safonov, 1996, Robust Control Toolbox User Guide, Natick, MA: The Math Works Inc.